SUBSYNCHRONOUS VIBRATION OF MULTISTAGE CENTRIFUGAL COMPRESSORS FORCED BY ROTATING STALL

J.W. Fulton
Exxon Research and Engineering Co.
Florham Park, New Jersey 07932

A multistage centrifugal compressor, in natural gas re-injection service on an offshore petroleum production platform, experienced subsynchronous vibrations which caused excessive bearing wear. Field performance testing correlated the subsynchronous amplitude with the discharge flow coefficient, demonstrating the excitation to be aerodynamic. Adding two impellers allowed an increase in the diffuser flow angle (with respect to tangential) to meet the diffuser stability criteria based on factory and field tests correlated using the theory of Senoo (for rotating stall in a vaneless diffuser, Ref. 1). This modification eliminated all significant subsynchronous vibrations in field service, thus confirming the correctness of the solution. Other possible sources of aerodynamically induced vibrations were considered, but the judgment that those are unlikely has been confirmed by subsequent experience with other similar compressors.

INTRODUCTION

This paper describes the joint efforts that a manufacturer and a user made to solve a vibration problem. The vibration was caused by a rotating aerodynamic stall, which created a forced vibration of the rotor resulting in reduced bearing life. The compressor operates at a high pressure typical of natural gas re-injection service. The primary objective of this paper is to provide sufficient engineering information to be useful to others faced with similar problems, in the field, and during design. This objective includes relating the observed phenomena with theories of rotating stall. A secondary objective is to caution purchasers and users of high pressure centrifugal compressors about the potential consequences of rotating stall.

The paper is written from the equipment user's point of view, however it contains technical input from the manufacturer. Except as noted, the calculations of internal flow angles were made by Leon Sapiro of Solar Turbines Inc., who also contributed many valuable insights, and played a major role in solving this problem. Research by the manufacturer is reported in another paper presented at this workshop by Fozi (Ref. 2)

The main parts of the paper describe the following: the equipment, the vibration and its consequences; the method of field diagnosis; the internal analysis to identify the components responsible; the solution and results; an evaluation of the possible causes, including information from a similar case; and finally an empirical guideline indicating when serious vibrations will

result from rotating stall.

SUBJECT COMPRESSOR RE-INJECTS NATURAL GAS

The problem occurred on the high pressure casings of seven compressor trains used on four oil production platforms located in the South China Sea. Three of the platforms have two trains while the fourth has a single train. The manifestations of the problem were the same on all high pressure casings. The designs of three pairs of trains were similar. The fourth pair of trains were of an earlier type design, which had 178 mm (7 inch) diameter impellers, instead of the 190 mm (7.5 inch) impellers of all the rest. One train, of the newer design, was chosen as a prototype to concentrate efforts toward a solution.

Figure 1 shows the rated conditions of the chosen train. Natural gas, separated from the crude oil produced, enters the low pressure casing at 2070 kPa (300 PSIA). The high pressure casing takes suction at the interstage pressure of 5850 kPa (860 PSIA) and discharges the gas at 14480 kPa (2100 PSIA), to the re-injection wells.

CHARACTERISTICS OF THE VIBRATION

Figure 2 shows the vibration spectrum taken from the shaft proximity probe mounted vertically at the discharge end bearing. The subsynchronous vibration is typical of our case; 33 microns (1.288 mils) peak-to-peak at 27.5 Hertz. The 307 Hertz component is at running speed. All the spectra in this paper, unless otherwise noted, use 16 averages, to give representative amplitudes. The amplitude of the subsynchronous vibration fluctuates appreciably.

The operating conditions for Figure 2 were practically at the rated point of the high pressure casing; the speed 18420 RPM, the suction volume flow 470 cubic meters per hour (277 ACFM), and the suction and discharge pressures 6100 and 14600 kPa (885 and 2121 PSIA) respectively. The molecular weight was 21.4 averaged from several gas samples, compared to 24.0 rated.

The subsynchronous vibration frequency is about 9 percent of RPM, which is typical of the aerodynamically forced type. Bonciani and his co-workers (Ref. 3) provided some of the first descriptions of shaft vibrations in high pressure compressors which were attributable to rotating stall. A comparison of their spectra to Figure 2 showed that it was similar. They emphasized that rotating stall caused a forced subsynchronous vibration as opposed to its being a self-excited resonant subsynchronous vibration.

Figure 3 shows the vibration spectrum taken at the suction end bearing. These data were collected concurrently with Figure 2. The suction end subsynchronous vibration levels were less than 12 microns (0.5 mils) for all operating conditions tested.

The low pressure casing also showed traces of subsynchronous vibration at frequencies associated with "aero-forced" vibration. Figure 4, which uses a logarithmic scale to make the small amplitude vibrations appear more prominently, shows two such frequencies, one with an amplitude of 2 microns (0.08 mil) at 25 Hertz, and another (not marked) next to it with a frequency of 55 Hertz. (The other subsynchronous peak, marked 0.1 mil at 145 Hertz is at a frequency near the first lateral critical speed of the rotor and is probably a "self-excited" vibration.) The subsynchronous vibration of the low pressure casing was always small in amplitude.

CONSEQUENCES OF THE VIBRATION

The subsynchronous vibration was not limited to the 33 microns (1.288 mils) shown in Figure 2. As running time increased the vibration amplitude at the discharge end bearing would increase to the 50 micron alarm level and on to the 63 micron protective shutdown. Forced shutdowns resulted, requiring discharge bearing replacement before starting up again.

To put the magnitude of the problem in proper perspective, it must be pointed out that the subsynchronous vibration was sufficiently limited in amplitude to allow commissioning and operation of the compressor without incident, except for abnormal bearing wear requiring frequent bearing replacement. From the equipment operator's viewpoint, the consequences of such a non-resonant forced response are less severe than the resonant and self-excited type of subsynchronous vibration, which can have a catastrophic consequence on operability. (For instance see Ref. 4.)

Bearing Wore at Pivot Pins

Figure 5 shows the bearing wear pattern. The pivot pin, which supports the pad in the carrier, wears into its mating surface in the back of the bearing pad. The extent of the worn area matches the length of the pin. The depth of the wear into the pad was typically 25 microns (1 mil) on the most severely worn pad, as found when the bearing was removed due to excessive subsynchronous vibration. The overall diametral clearance typically increased to approximately 4 mils at that time compared to the 2.7 mils maximum allowable clearance for a new bearing.

Primarily as a result of the subsynchronous vibration causing bearing wear, the median bearing life was 1000 hours (with a minimum of 88 and a maximum of 2200 hours) for all seven high pressure casings, during the year this problem was under study. This impacted adversely on the availability of the compressor trains and justified considerable effort for correction.

The increase in vibration due to bearing wear can be related to a corresponding reduction in bearing stiffness and damping. The bearing would wear to approximately 4 mils (before a bearing change was required), causing the stiffness and damping of the bearings to decrease substantially. The reduced

stiffness allowed the subsynchronous vibration amplitude to increase correspondingly. The manufacturer has performed rotor response analyses which show a 4.4 times increase in response sensitivity when the bearing clearance is increased from 2 to 4 mils (diametral). This reduced stiffness allowed the once-per-revolution component to increase as similarly, but the effect is not so pronounced here because the ratio of increase is partially masked in this case by the presence of a spurious amplitude due to shaft imperfections adding to the once-per-revolution component.

Problem Associated with the Discharge End of the High Pressure Casing

The bearing wear-out, due to the fretting of the tilting pads at the pivot pins, occurred predominantly on the discharge end of the high pressure casing. The subsynchronous vibration also occurred predominantly on the discharge end, as can be seen by comparing Figures 2 and 3. A detailed investigation, including metallurgical laboratory studies of the worn bearings, did not reveal any other supportable cause of the pivot fretting. The suction end pivots did not wear out prematurely.

The bearing life of the low pressure casing has not been a problem. Although detailed records were not kept in the absence of any problem, at least one of the low pressure compressors is still using its original bearings after 17000 hours of service. As the low subsynchronous vibration amplitudes of Figure 4 are typical, the correlation of pivot wear with high subsynchronous vibration amplitudes is thus complete.

Damage Criteria

Because the subsynchronous vibration occurred at low frequency, the shaft vibration velocity, due to this component, was low (about 3.5 millimeters per second, equal to 0.14 inch per second) compared to the 6.3 mm/s (0.25 in./sec.) maximum acceptable for a compressor in good condition. Therefore the manufacturer initially believed that the subsynchronous vibration was not harmful. The manufacturer placed a filter in the vibration monitor system of one of the other compressors of similar design to suppress the subsynchronous vibration signal. Since the compressor was no longer limited by the vibration shutdown from running with high levels of subsynchronous vibration, the result (due to bearing wear) was an increase in both the subsynchronous vibration and the once per revolution vibration, which eventually caused excessive labyrinth wear.

The API 617 limit on non-synchronous components of shaft displacement amplitude (peak-to-peak) specifies that the subsynchronous vibration be less than 4 microns (0.16 mils); the specification limits such components to 10 percent of the overall allowable vibration. The overall allowable vibration in mils equals the square root of [12000 / maximum continuous RPM]. This limit is safe, based on the good experience with the low pressure casings.

Damage Mechanism Hypothesis

The mechanism of the bearing pivot-pin wear is believed to be caused by the subsynchronous vibration breaking down the load-carrying oil film between the pivot-pin and the back of the bearing pad. The subsynchronous vibration tends to hold the the pad against its pivot, thus squeezing out the oil film, while the once-per-revolution component causes the fretting motion. The cause of the fretting is analogous to the wear that occurs on a reciprocating compressor wrist pin having no load reversal.

FIELD DIAGNOSIS

In the field or in testing compressors purchased for a commercial project, transducers for dynamic pressure or velocity usually can not be placed inside the casing. Therefore, diagnosis of aerodynamically induced subsynchronous vibration outside the research laboratory must depend on analysis of commonly available data such as vibration or pressures, temperatures and flows measured outside the casing flange boundaries.

Spectral Characteristics

Field diagnosis is simplified by the distinctive patterns observable in the spectrum. In most cases reported in the literature, rotating stall in stator components has occurred at 4 to 20 percent of RPM. With the spectral analyzer in the real time mode, it can be seen that the component frequency is not locked on to an exact fraction of the rotor speed, but fluctuates slightly, as does the amplitude. In the present case, many distinct frequencies could be produced at will by varying the flow slightly at constant speed. For instance, decreasing the flow from 593 to 562 cubic meters per hour (349 to 331 ACFM) caused the 27.5 Hertz component to split into 12.5 and 40 Hertz components. This phenomena is believed to be due to different numbers of stall cells forming in various stages, but without transducers inside the casing, neither the exact number of cells nor their location can be identified.

Correlation with Flow Coefficients

Once the spectra identified the nature of the problem, we took the second step essential in diagnosis of an aerodynamic stall problem. An aerodynamic performance test was made at full pressure, speed and gas density, measuring the subsynchronous vibration at each point, so that the subsynchronous vibration could be correlated with the performance. The good correlation of subsynchronous vibration with the flow coefficient (proportional to volume flow divided by RPM) showed that the vibration was aerodynamically induced. Later, the results of this test were used to calculate the internal flow angles occurring at the inception of the subsynchronous vibration.

The results of correlating subsynchronous vibration with the flow coefficients from the field test are shown in Figures 6 and 7. Figure 6 shows

that the subsynchronous vibration correlates very well with the discharge flow coefficient (based on the discharge flange volume flow). Figure 7 shows that the subsynchronous vibration correlates less well with the suction flow coefficient. The two flow coefficients do not form a constant ratio to each other, because the test was run at two different speeds, causing the volume ratio across the compressor to vary at similar inlet flows. The result of this difference in volume reductions can be seen in Figure 7, where the 17200 RPM data (squares) forms a distinctly different curve from the 18450 RPM data (circles). The better correlation at the discharge end suggests that the suspected stall is in the final stages instead of the initial stages.

The rated flow is indicated on the flow coefficient scale of Figures 6 and 7. It can be seen that the subsynchronous vibration, which is usually associated with operation near the compressor surge line, begins in this case at flows over thirty percent larger than rated (suction basis).

The theory that the final stages are responsible is supported by the predominance of the subsynchronous vibration at the discharge end compared to the suction end. Other investigators (Ref. 3) have used asynchronous vibration response calculations to help identify the location of the stalled stage by comparing the ratio of the subsynchronous vibration at the suction and discharge ends.

INTERNAL ANALYSIS

The result of the field diagnosis was a correlation of the subsynchronous vibration with the exit flow coefficient. Although this demonstrates the cause to be aerodynamic, further analysis is required to determine which component is responsible. The basic strategy for identifying the component is to calculate the flow angles inside the compressor, for the flow measured in the field at the inception of the subsynchronous vibration. These calculated flow angles must then be correlated with the critical flow angle for rotating stall of each of the suspected components. The critical flow angle for rotating stall must be known from calculations based on theory, or from empirical correlations made when sufficient transducers were installed in the compressor flow passages to identify the component which initiated the rotating stall. Even with extensive internal instrumentation, it is not a trivial problem to prove which component is responsible for the rotating stall, as is apparent from References 5, 6 and 7.

Based on internal instrument measurements in another compressor at the manufacturer's plant (Ref. 2), the prime suspect was rotating stall in the diffuser. Other possibilities concerned us, especially rotating stall due to the deswirl vanes after the diffusers, based on a paper by Bonciani (Ref. 8). This and other possible causes of the subsynchronous vibration will be discussed later in this paper. Figure 8 is a cross section of the discharge end of the subject compressor, showing the vaneless diffusers and the deswirl vanes.

Internal Transducer Test Results

The manufacturer tested the other compressor at the factory, with pressure transducers mounted in the last stage diffuser, using full pressure in a closed loop (Ref 2.) Full gas pressure, or more fundamentally, full gas density, is necessary to produce the same gas forces and thus the same shaft vibrations as observed in the field. Of course the same conditions of dynamic similitude (mainly volume flow to speed ratio and volume reduction across the casing) must be observed, as in performance testing, to produce the same flow angles throughout the compressor. Oscilloscope traces of pressure fluctuation versus time from the two transducers are interpreted in Figure 9 for two different flows. At the higher flow, the trace shows mainly high frequency flow noise and impeller vane passing frequencies. As the angle of flow into the diffuser is reduced, with respect to tangential, an 8 psi (peak-to-peak) stall cell is formed. The 75 degree angle between the two transducers shows that a single cell is rotating in the same direction as the shaft. The frequency of the propagation is 10 Hertz (labeled 1/1800 RPM). Although not shown here, as the flow is further reduced to a flow angle of 6.5 degrees, the stall forms two cells of unequal pressure with 80 psi (p-p) at 37.5 Hertz.

Senoo's Theory

This onset of diffuser stall can be correlated to the diffuser inlet flow angle, for a given diffuser aspect ratio b3/R3 (see definitions). Kinoshita and Senoo give such a correlation (Ref. 9), as do Ligrani, Van Den Braembussche and Roustan (Ref. 10). As can be seen in Figure 10, these correlations are very similar and practically identical in our range of interest. These correlations are based on theoretical calculations and compare favorably to empirically determined stability thresholds reported in the literature. Other factors having a secondary influence are radial and tangential distortion of the inlet flow from the impeller, plus the Mach and Reynolds numbers, all of which have been quantified in a theoretical investigation (Ref. 11).

The points labeled with the subsynchronous vibrations amplitudes in Figure 10 compare the last diffuser inlet flow angles, near the inception of subsynchronous vibrations, to two rotating stall criteria. Several points at various flow angles are shown to allow the reader to evaluate the inception point versus the level of vibration he considers significant. Presuming, on the evidence above, that the stall is occurring in the last stage, the agreement is fair. Choosing the smallest vibration shown (5 microns or 0.19 mils) as the inception point, results in the criteria being optimistic by nearly four degrees, with the actual inception occurring at 13 degrees versus 9 predicted.

These flow angle calculations, for the last stage, were made by the author, based on the performance test data from the field. One dimensional compressible flow calculations were used, knowing the state and flow at the discharge flange, the geometry of the impeller tip plus diffuser, and the impeller speed. The diffuser static pressure recovery coefficient was estimated

at 0.46, the slip factor at 0.88, and the impeller tip boundary layer (displacement) blockage at 0.95. Labyrinth leakages were calculated. In this compressor, flow is drawn off before the discharge flange and injected into the balance piston labyrinth two teeth away from the last impeller. The draw off and the flow up the back of the impeller, as well as the flow from the tip down the shroud to the eye were accounted for. This calculation method reflects actual volume ratios, but is only possible for the last stage. The vendor used an internal flow analysis refined by many factory tests to calculate the other flow angles quoted in this paper; these were not adjusted for the minor differences in observed volume ratio, but are reliable by virtue of extensive and critical use. The vendor's flow angles were smaller by typically two degrees, thus agreeing with the stall criteria more closely, being about two degrees larger than the predicted critical angle, for the last stage.

The mechanism of rotating stall in a vaneless diffuser is due to unsteady flow in local areas of the diffuser. According to Senoo, it is a phenomena of the boundary layer flow along the diffuser walls. Figure 11 shows the behavior of the boundary layer on the diffuser walls at the threshold of stability according to the theoretical model of Reference 1. The flow angles of the core flow and the boundary layers on the diffuser walls (the walls are identified with respect to the disk and shroud of the preceding impeller) are plotted as a function of the ratio of the local radius to the diffuser inlet radius. The flow angles are defined so that a purely tangential flow would have an angle of zero. It can be seen that, at first, the disk-side boundary layer reverses direction and "falls" back toward the impeller under the influence of the adverse pressure gradient normally existing in the diffuser. Then further along, the shroud-side boundary layer falls back. Reference 1 states "... a reverse flows occurs on the two walls alternately. Such a phenomena has not been observed in two-dimensional or conical diffusers and intuitively it is difficult to understand. The phenomena is related to the complicated nature of the flow, where the two wall boundary layers exchange momemtum so that each boundary layer satisfies the equations of motion in the radial and tangential directions which include the centrifugal force and the wall friction force."

Just as a reminder, rotating stall is not the same as a complete breakdown in flow, which would cause compressor surge. When compressor surge occurs, all areas of the flow reverse. (The flow meter upstream of the suction flange will momentarily show zero flow during a full surge cycle.) For Figure 11 the core flow is still carrying a net flow in the normal direction.

FLOW ANGLES INCREASED BY ADDING STAGES

To solve the rotating stall problem the manufacturer re-staged the high pressure compressor from six impellers to eight, causing the operating point to be much further from surge. This was done by adding two standard modular stages having a reduced design flow coefficient. The new staging caused the flow angles in the diffuser to be more radial, thus avoiding the critical angle for diffuser rotating stall. Another possibility, stall due to the deswirl vanes,

was addressed as a contingency measure, and will be discussed later.

Table 1 compares all stages of the original and re-staged high pressure casing to a diffuser stability criterion used by the manufacturer. The manufacturer's flow angles, from an internal flow calculation, are used as well. This criterion is identical to van den Braembussche (Ref. 10), except that 2 degrees are added to the criterion for the last stage, to account for its observed sensitivity. The row labeled "stall" indicates whether each stage is expected to experience diffuser rotating stall at the rated conditions. A dash indicates that the stage is at the threshold of stall.

The flow angles entering the diffuser are given first for the original design at rated flow. The original design had six impellers and diffusers. The flow entered the first diffuser at an actual angle equal to eight degrees. The next stage was a narrower type, which causes the flow angle to be larger, here eleven degrees. The succeeding four diffusers were the same width as well, and the flow angle decreased one degree per stage, due to the compression of gas. The stall criterion angle is twelve degrees for the first diffuser, which is the wider. The criterion gives ten degrees for the stages two through five, which all have the same width. Even though the last stage width is the same as the preceding stage, its criterion is two degrees larger, based on the factory test of the internally instrumented compressor. The actual angles of stages one, four, five, and six fall below the criterion, indicating rotating stall in those stages. The forces due to the stall increase with pressure. Thus the stall induced vibration is predicted to predominate on the discharge end of the compressor.

The solution to the rotating stall was to re-stage by adding two impellers and diffusers. These had narrower flow passages than the preceding stages, thus giving larger flow angles. At rated flow, the actual flow angles for the new stages seven and eight are thirteen and twelve degrees respectively. Because the load is now shared by more impellers, the first six now operate at a somewhat larger flow coefficient. As a result, the actual flow angle increases three degrees on average for the first six stages, compared to the original staging. Now the actual angles exceed the criteria for all stages except the first. Stall of the first stage was not readily avoidable with the staging available, and was accepted on the basis that subsynchronous vibration had not been a practical problem on the suction end of this compressor.

One unusual aspect of the staging used should be mentioned, because it helps explain why these stages exhibit rotating stall at flows considerably in excess of rated flow. The diffuser width is 26 percent greater than the impeller tip width for the stage designated type "A" stage and 15 percent on the type "B". The extra width of these diffusers, compared to more conventional designs, causes the flow angles to be more tangential, and thus more prone to rotating stall. Narrower diffusers are now being manufactured for the high pressure casings on the other three platforms. Among other manufacturers throughout the industry, typical re-injection compressor practice is to design the diffuser

widths in the order of 0 to 35 percent less than the impeller tip width.

Results of Re-Stage

The results of the design change were completely successful, as shown by the spectra in Figure 12. The re-stage reduced the subsynchronous vibration to only 2 microns (0.07 mil) at 45 Hertz. These spectra were taken at more than rated pressure and near the actual surge line, which was determined during this test. Operation at 2500 psi discharge pressure and near surge was made as a proof test. No significant subsynchronous vibration was evident at stall frequencies (or any other frequency) on the high pressure casing. Previously 2100 psi with a larger margin to surge had been the limit.

One year (8000 hours operation) has now passed without any indication of reoccurrence of the bearing wear-out problem. Previously 2200 hours operation was the longest bearing life.

SUBSEQUENT CASE CORRECTED BY NARROWING THE DIFFUSERS

After the re-stage, two other compressor trains from the same manufacturer having the same design and frame size were purchased. The train layout was the same as Figure 1; the internal design of the high pressure casing the same as Figure 8. Because of the previous experience, the specified performance test (American Society of Mechanical Engineers Power Test Code - 10) was conducted as near to rated pressure as possible, to detect any significant subsynchronous vibration forced by rotating stall.

Both the high and the low pressure casings of both trains showed vibration typical of rotating stall. On the low pressure casings, the subsynchronous vibration was within the API 617 limit of 3.7 microns (0.15 mils) when operating at rated pressure. On the high pressure casings the subsynchronous vibration was near the API limit, even though the suction pressure of the test was approximately half the rated pressure. Correction was required because there was no way to demonstrate, due to suction pressure limits with this test facility, that the vibration at full suction pressure would be within the API limit. To move the stall inception point to lower flows, the manufacturer installed narrower diffusers in all stages of the high pressure casings.

Table 2A lists the vibrations observed, while Table 2B lists the flow angles of the stage presumed stalled, and the flow as a percentage of the surge flow. In both tables column "A" is the point that encroached on the API limit. Columns "B" are for a flow 29% above surge, near rated flow, which was 32% above surge. Column "B" of Table 2B predicts stall, with the fifth stage 0.9 degrees below the critical flow angle; small stall induced vibrations resulted. The second compressor was not tested with wide diffusers. Column "D" shows that narrow diffusers on the first compressor moved the stall inception from 29% to 19% above surge flow .

The second compressor, with narrow diffusers, had larger subsynchronous vibrations than the first did with wide diffusers, as shown in column "E". However the narrow diffusers on the second restricted the flow where large vibrations occurred to 13% above surge, allowing the surge protection system settings to exclude this stall from the operating range. The inception point, column "F", shows that the stall criteria predicted the stall should not occur for another 0.4 degrees.

The aerodynamic performance was practically unaffected by the narrower diffusers. The head and efficiency were unchanged at the rated point. The head versus flow curve was only slightly changed. Examining the row "Rated flow % above surge" shows that the surge flow is unchanged between columns "A" and "D"; thus surge was unchanged by the narrower diffusers in this case.

Table 3 shows the ratio of the diffuser width (b3) to the impeller tip width (b2) for both the original and revised diffusers. The original diffusers were unusual in being wider than the impellers, with the last stages, which are of a lower specific speed, having the largest ratio. The revised diffusers have a uniform ratios of ordinary proportions.

That the narrower diffusers were successful in eliminating rotating stall in this case is significant. Manipulating the principle variables, diffuser inlet flow angle and diffuser aspect ratio (b3/R3), while making no other changes, supports the theory that the stall criteria in Figure 10 is sufficient to predict diffuser rotating stall inception, (accounting, where necessary, for inlet flow distortion plus Mach and Reynolds number effects.) Other theories were considered, as discussed below, but an evaluation was difficult without the evidence from the narrower diffusers.

WAS DIFFUSER STALL SOLELY RESPONSIBLE?

Both the stator and the rotor can be responsible for rotating stall phenomena in centrifugal stages with vaneless diffusers (Ref. 5 and 6.) Frigne and Van Den Braembussche found five distinct stall characteristics in one single stage test compressor, three due to the impeller and two due to the diffuser. Table 4, adapted from their work (Ref. 6) summarizes these characteristics. Stator components other than the diffuser alone can have an influence, as we shall now discuss.

Influence of Deswirl Vanes Considered

Careful experiments by Bonciani and Terrinoni (Ref. 8) have shown that, in some industrial centrifugal compressor configurations, rotating stall type pulsations in the diffuser area can be induced by the return vanes interacting with the flow. The critical incidence angle with respect to the leading edge of the return vane mean camber line was found to be 6 to 8 degrees for the particular stages tested (defined so the incidence is increasing with

decreasing flow).

A photograph of the return vanes, taken during the re-staging of the South China Sea compressor, is given in Figure 13 to show the form of the vane leading edges, which are of a type tolerant to a wide range of incidence. Figure 14 shows the incidence angle, with respect to the leading edge mean camber line, for the fifth stage before re-staging. As can be seen, there is no stall induced vibration for incidences less than 11 degrees, and strong vibrations do not appear until the incidence exceeds 15 degrees. The incidence angles for the preceding stages are similar. No change was made to these vanes, because the vendor did not believe the return vanes were the cause of the rotating stall. Although the re-stage reduced the incidence angle by about two degrees, the angle at the return vanes still greatly exceeded the 6 to 8 degree criterion for rotating stall. Therefore violating this criterion does not cause stall in our case. Perhaps differences in stage geometry, compared to Reference 8, invalidate applying this particular incidence criterion.

Exit Vanes Modified

The last stage has 12 exit vanes, axially configured, indicated as the second set of "deswirl vanes" from the left in Figure 8. A cross section of two of these vanes, drawn to scale for both profile and spacing, is shown in Figure 15. The vanes are required for structural strength, and are not expected to recover any significant amount of energy from the gas tangential velocity before passing the flow to the discharge collector. The incidence angle on them was quite high, being 21 degrees at the rated point, shown as "I" in Figure 15. Due to some concern about the vane stall theory mentioned above, and because nothing was lost by doing so, these vanes were modified to blunt struts, as shown. The elimination of a definite leading edge, and of any flow turning capability, removed all possibility of the influence of these vanes on rotating stall.

The exit vanes were not made blunt on the subsequent case of rotating stall, corrected by narrowing the diffusers. As discussed, narrowing the diffusers, only, was sufficient to eliminate the stall. The incidence angle on the exit vanes was only slightly improved over the case in the previous paragraph. Therefore we conclude that the poor incidence on the exit vanes did not cause the stall.

Inducer Stall Criteria Respected

Following the argument of Kinoshita and Senoo in Reference 9, the impeller inducer inlet incidence and the impeller diffusion ratio (w2/w1) were calculated to evaluate the possibility of the impeller causing the rotating stall. The vendor examined one case, the last stage of the high pressure casing, the one which has 7 inch diameter impellers as mentioned earlier. The principle difference between this design and all the others in this paper is that the hub-to-tip diameter ratio is smaller; 0.36 versus 0.52 on the other compressor designs. The vendor calculates that the incidence angle at the shroud is 2.5

degrees at the rated point of the compressor train and 5.7 at surge. This compressor vibrates due to rotating stall, with the severity increasing as flow is decreased toward the rated point. Our incidence of less than 5 degrees makes it unlikely that last stage impeller stall is responsible for the vibration, based on comparison to the 12 degrees inducer incidence (at the RMS radius) at impeller stall, reported by Frigne and Van Den Braembussche in Reference 11, and the 13 degrees (at shroud) reported by Kammer and Rautenberg in Reference 5. The velocity ratios (w2/w1RMS) are 1.27 at rated flow and 1.43 at surge, which should be within the diffusion capability of the impeller.

The case where the rotating stall was moved to a predictable lower flow by narrowing all the diffusers, with no other changes, gives additional support to the hypotheses that inducer stall is not generally responsible for the rotating stall induced vibrations described in this paper.

PREDICTING VIBRATION AMPLITUDES

Rotating stall should be kept out of the operating range where practical, but in many cases this may be neither necessary nor economic. For instance the low pressure casings discussed above have rotating stall, based on their vibration spectra, but the vibration amplitudes are not harmful, so there is no incentive to eliminate the stall. When purchasing a compressor there is a need to know whether rotating stall will be a potential problem which should be addressed before it runs at rated conditions in an operating plant. For this, and other purposes, a criterion for the vibration amplitude due to stall is useful.

From the equipment user's point of view, such a criterion should indicate where concern about stall induced vibration begins. Therefore the criteria should err toward over-estimating the vibrations amplitude. Although accuracy is advantageous, it is not paramount because once the concern is raised, any particular case will have to be settled by reference to the experience of the particular manufacturer involved. Of course some compressors may then be found acceptable even though they exceed such a criterion.

Criqui has published an empirical criterion for the vibration severity of rotating stall for the compressor designs discussed in this paper (Ref.12.) His plot may not be accurate when applied to dissimilar compressor designs. Figure 16 shows his line, with points added from the cases discussed in this paper. The criterion predicts significant subsynchronous vibrations for stages which operate with diffuser rotating stall (expected where the diffuser entry flow angle fails to meet the criteria in Figure 10) and which have stage pressure ratios and stage discharge pressures plotting above and to the right of the line . The added points are for the compressors discussed in this paper. These points refer to vibration above the limits of API 617, a more stringent standard than Criqui's line, which reflects operator complaints. His criterion does not take into account where the particular stage is located along the shaft, nor how many stages are stalled simultaneously.

TESTING FOR ROTATING STALL INDUCED VIBRATIONS

Compressors specified to petroleum industry standards are not usually tested at the manufacturer's works for rotating stall induced vibrations meeting the previously mentioned API limit. The API 617 mechanical test has nothing to do with aerodynamic similtude. Nor does it specify the correct frequency range to find most rotating stalls. The frequency range inspected is 0.25 to 8 times running speed (API 617 item 4.3.4.4 paragraph 1.). Furthermore the usual aerodynamic performance test, conducted according to ASME PTC-10, cannot be expected to induce significant vibrations because it is usually conducted at reduced pressure compared to rated. Although any stall in the flow range should be present during a performance test, usually no internal instrumentation is provided which would discover rotating stall.

LESSONS LEARNED

The main points of this case can be summarized as follows:

1. Tilt pad bearings can suffer premature wear-out as a result of forced subsynchronous vibration, in spite of the relatively low vibration velocity of the shaft motion. The displacement amplitude of the subsynchronous vibration (0.17 mils) at the start of the wear-out process, when a new bearing was installed (shown in Figure 6), was just slightly less than the API Standard 617 limit for subsynchronous vibration.

2. The Senoo and Van Den Braembussche criteria were closely confirmed by both the field and the factory test correlations of subsynchronous vibration with the diffuser flow inlet angle. When the criteria were respected, then the subsynchronous vibration was eliminated.

3. A rated pressure, rated gas density performance test, maintaining rated ACFM/RPM and rated volume reduction across the casing is required, if this type of subsynchronous vibration problem is to be demonstrated during factory testing of new compressors. The rated pressure and density are required to produce the full subsynchronous vibration amplitude. The aerodynamic similitude is necessary to reproduce the gas flow angles throughout the compressor as required to respect the stall criteria.

The API 617 limits on vibration amplitude should be specified for any such test. However, the frequency range should be revised to include frequencies lower than the arbitrary 25 percent minimum in API 617. Both limits should be required of field operation as well.

The subsynchronous vibration problem does not have the same catastrophic effect on operability as does subsynchronous instability, and in the case described in this paper, merely degraded the compressor's availability. Therefore the cost of such a test should be weighed against the magnitude of the

potential problem. The empirical severity criteria may aid the evaluation.

4. Designs of new compressors should be reviewed against the rotating stall criteria, where the stage pressure and pressure ratios approach those of this case. Similar criteria are needed for components, other than diffusers, susceptible to rotating stall.

REFERENCES

1 Senoo, Y., Kinoshita, Y., and Ishida, M., "Asymetric Flow in Vaneless Diffusers of Centrifugal Blowers," ASME Journal of Fluids Engineering, March 1977, pp. 104-114.

2 Fozi, A. A., "An Examination of Gas Compressor Stability and Rotating Stall", Fourth Workshop on Rotor Instability Problems in High Performance Turbomachinery, Texas A&M University, June 1986.

3 Bonciani, L., Ferrara, P.L., and Timori, A., "Aero-Induced Vibrations in Centrifugal Compressors," Quaderni Pignone 29, June 1980 pp. 5-12.

4 Fulton, J. W., "Full Load Testing in the Platform Module prior to Tow-Out: A Case History of Subsynchronous Instablility," NASA Conference Publication 2338, May 28-30, 1984, pp.1-16.

5 Kammer, N., and Rautenberg, M., "A Distinction Between Different Types of Stall in a Centrifugal Compressor Stage," ASME Journal of Engineering for Gas Turbines and Power, Vol. 108, January 1986, pp. 83-92.

6 Frigne, P., and Van Den Braembussche, R., "Distinction Between Different Types of Rotating Stall in a Centrifugal Compressor With Vaneless Diffuser," ASME Journal of Engineering for Gas Turbines and Power, Vol 106, April 1984, pp. 468-474.

7 Abdelhamid, A.N., Colwill, W.H, and Barrows,J.F., "Experimental Investigation of Unsteady Phenomena in Vaneless Radial Diffusers," ASME Journal of Engineering for Power, Vol. 101, January 1979, pp. 52-60.

8 Bonciani, L., and Terrinoni, L., "Influence Of Stationary Components on Unsteady Flow in Industrial Centrifugal Compressors," NASA Conference Publication 2338, May 28-30, 1984, pp. 429-479.

9 Kinoshita, Y., and Senoo, Y., "Rotating Stall Induced in Vaneless Diffusers of Very Low Specific Speed Centrifugal Blowers," ASME Paper No. 84-GT-203, June 1984.

10 Ligrani, P.M., Van Den Braembussche, R., and Roustan, M., "Rotating Stall Measurements in the Vaneless Diffuser of a Radial Flow Compressor," ASME Paper No. 82-GT-257, May 1982.

11 Senoo, Y., and Kinoshita, Y., "Influence of the Inlet Flow Conditions and Geometries of Centrifugal Vaneless Diffusers on Critical Flow Angle for Reverse Flow," ASME Transactions, Vol. 99, No. 3, March 1977, pp. 98-103.

12 Criqui, A. F., "Advancements in Centrifugal Gas Compressor Stability," Solar Technology Seminar '86, San Diego, California, February 5-8, 1986, pp. 40-1 to 10.

13 Fulton, J. W., "Subsynchronous Vibration of a Multistage Centrifugal Compressor Forced by Rotating Stall," Solar Technology Seminar '86, San Diego, California, February 5-8, 1986, pp. 41-1 to 41-12.

NOMENCLATURE

ACFM - actual cubic feet per minute
API - American Petroleum Insitute
b2 - impeller tip width
b3 - diffuser width at the beginning of the parallel wall section
d - impeller diameter in inches
RMS - root mean square
RPM - revolutions per minute
R3 - diffuser radius at the beginning of the parallel wall section
w1 - relative flow velocity entering the impeller
w2 - relative flow velocity leaving the impeller

Flow coefficient = (700/d^3)*(ACFM/RPM)

Calculated Diffuser Flow Angles at Rated Flow

Stage	1	2	3	4	5	6	7	8
Old Staging								
Impeller Type	1C	2B	2B	1B	1B	1B		
Actual	8	11	10	9	8	7		
Criteria	12	10	10	10	10	12		
Stall	Yes	No	-	Yes	Yes	Yes		
New Staging								
Impeller Type	1C	2B	2B	1B	1B	1B	2A	2A
Actual	10	14	12	11	10	10	13	12
Criteria	12	10	10	10	10	10	8	10
Stall	Yes	No	No	No	-	-	No	No

AGX586-32

Table 1. Calculated Diffuser Flow Angles at Rated Flow

Subsequent Case: Wide and Narrow Diffusers
Subsynchronous Vibrations

	A	B	C	D	E	F
Diffuser Width	Wide	Wide	Wide	Narrow	Narrow	Narrow
Compressor No.	1	1	2	1	2	2
Discharge (mils)	0.14	0.04	Not	0.05	0.28	0.07
Suction (mils)	0.012	0.001	tested	0.001	0.05	0.023
Frequency (Hertz)	41	33		37	26	55
% Running speed	15.7	12.7		14.2	9.7	20.4

AGXF586-37

Table 2A. Subsequent Case: Vibrations Observed

Subsequent Case: Wide and Narrow Diffusers Diffuser Flow Angles

	A	B	C	D	E	F
Diffuser Width	Wide	Wide	Wide	Narrow	Narrow	Narrow
Compressor No.	1	1	2	1	2	2
Stages stalled	2,5	2,5	Not	2,5	2,6,7	2,7
Angle given for stage #	5	5	tested	5	7	7
Degrees above critical	-4.3	-0.9		-0.7	-2.5	0.4
% above surge flow	8.9	29		19	13	27
Rated flow % above surge	32	32		32	38	38
Test point no.	c40	c31		c41	f16	f13

AGXF586-38

Table 2B. Subsequent Case: Corresponding Flow and Diffuser Inlet Angles

Subsequent Case: Diffuser Width Changes

	Original Diffuser Tip Width Ratio*		Revised Diffuser Tip Width Ratio*	
Compressor Stage	1	2	1	2
1	1.05	1.06	0.85	0.84
2	1.05	1.06	0.85	0.84
3	1.06	1.15	0.84	0.85
4	1.06	1.15	0.84	0.85
5	1.06	1.15	0.84	0.85
6	1.15	1.15	0.85	0.85
7	1.15	1.15	0.85	0.85

*Ratio - Diffuser Width / Impeller Tip Width

AGSF586-33

Table 3. Subsequent Case: Diffuser Width Changes

Rotating Stall Characteristics

Type	Character	Amplitude*	No. of Calls	Harmonics	Freq. Ratio
Impeller	Mild	0.065	3,4,5	No	0.14
Impeller	Abrupt	0.30	1,2,3	N/A	0.26-0.31
Impeller	Progressive	0.10	1,2,3	Yes	0.67-0.81
Diffuser	High Freq.	0.10	3	No	0.17-0.21
Diffuser	Low Freq.	N/A	2	No	0.13-0.16

* Amplitude (in diffuser) = (Max. Vel.) / (2*RMS velocity

AGX586-34

Table 4. Characteristics of the Different Types of Rotating Stall as Tested on a Single Impeller Air Test Facility (Measured by Frigne and Van Den Braembussche, Ref. 6)

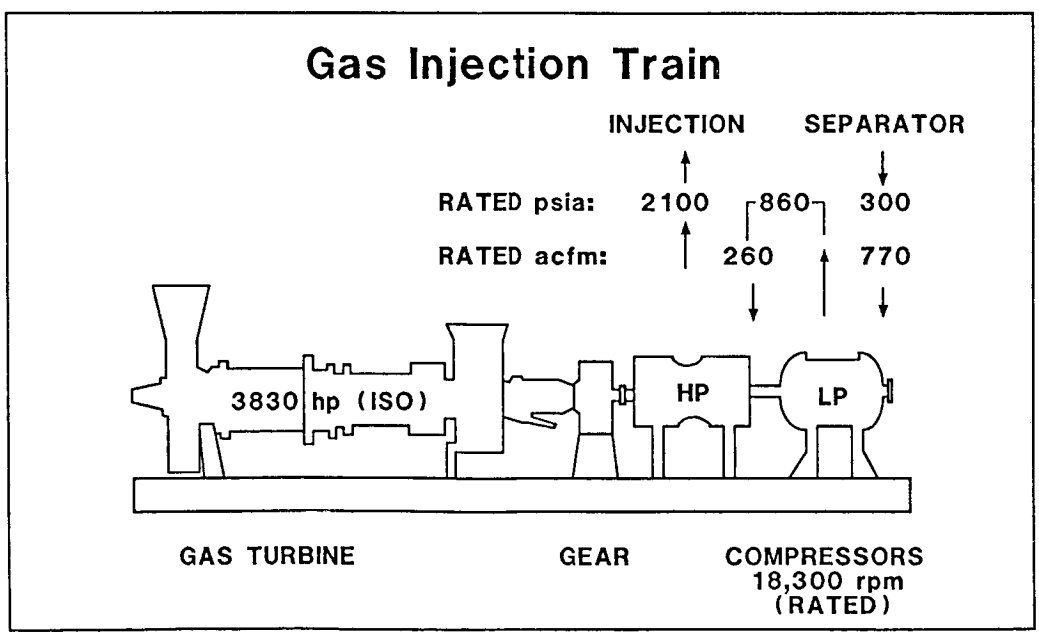

AGXF586-1

Figure 1. Compressor Train

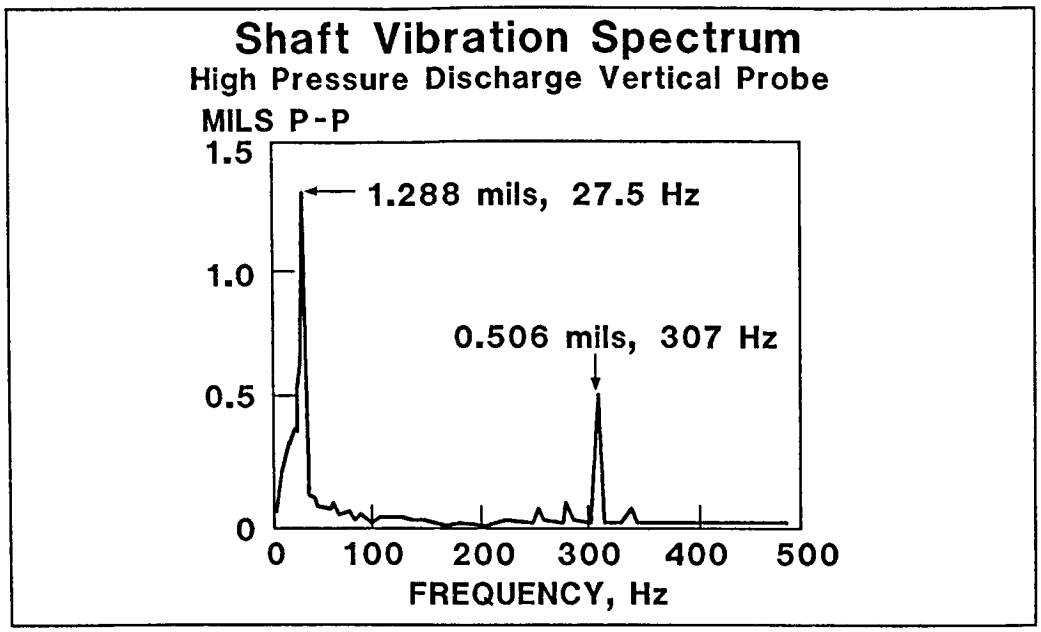

Figure 2. Proximity Probe Spectrum of the Problem Vibration

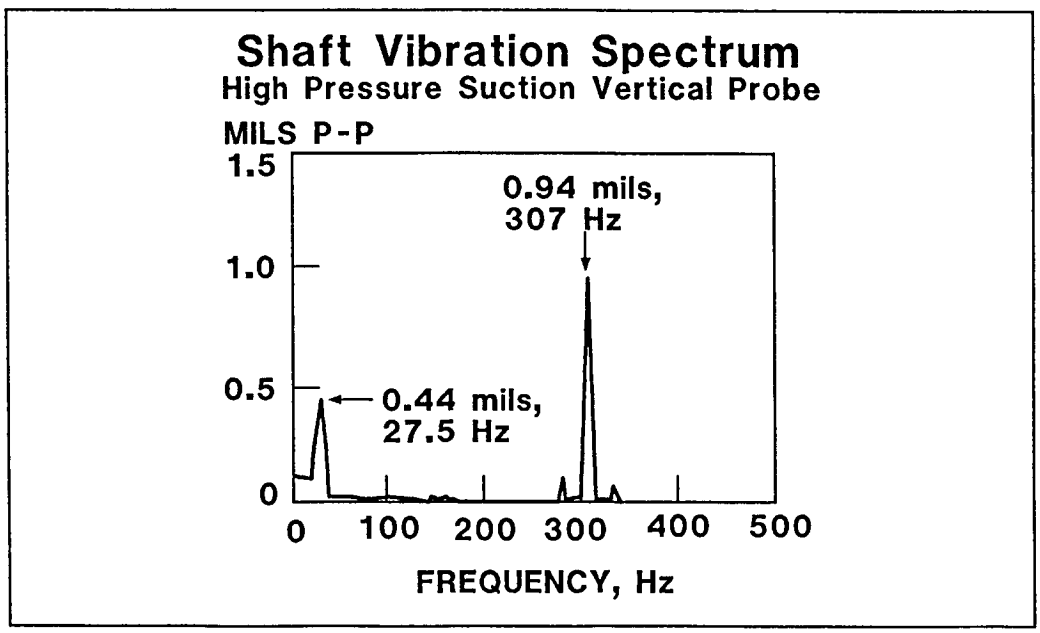

Figure 3. Spectrum at Suction End

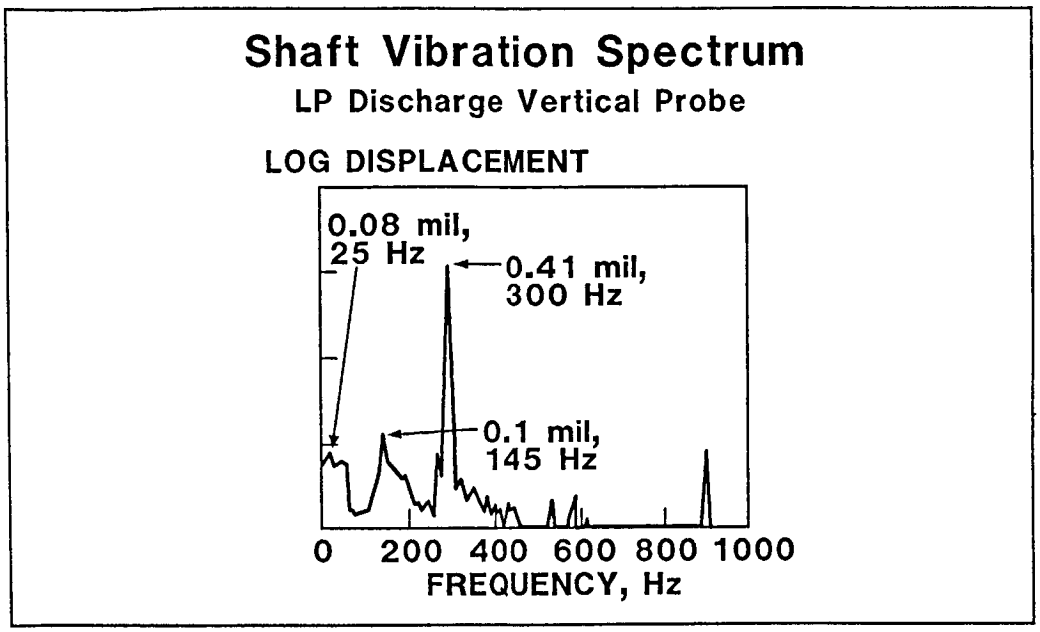

Figure 4. Spectrum from the Low Pressure Casing

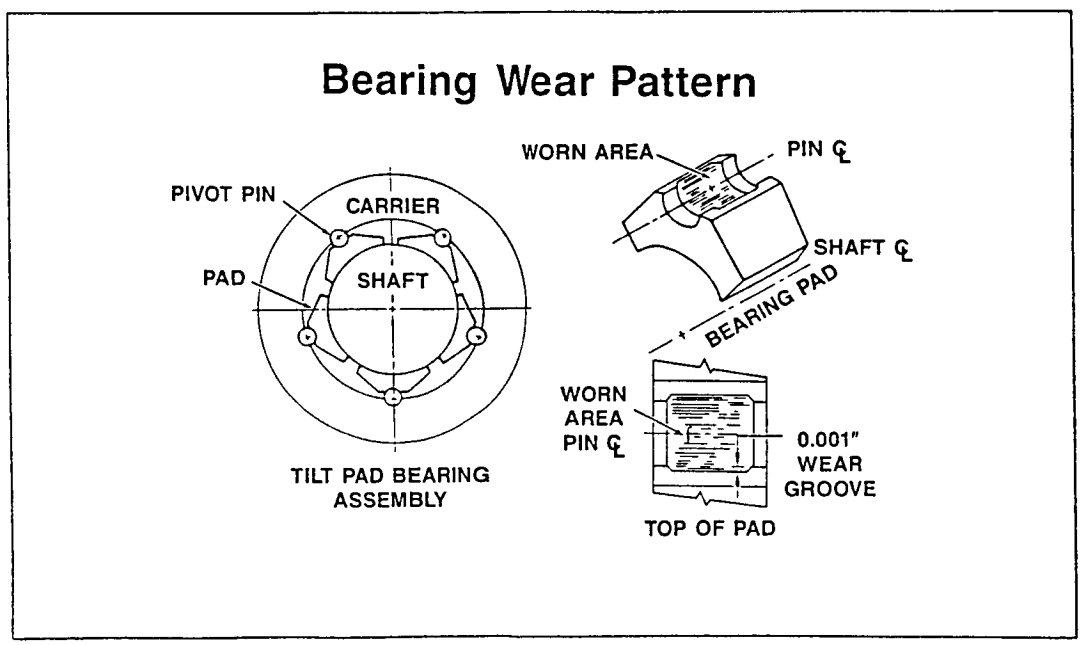

Figure 5. Bearing Wear Pattern

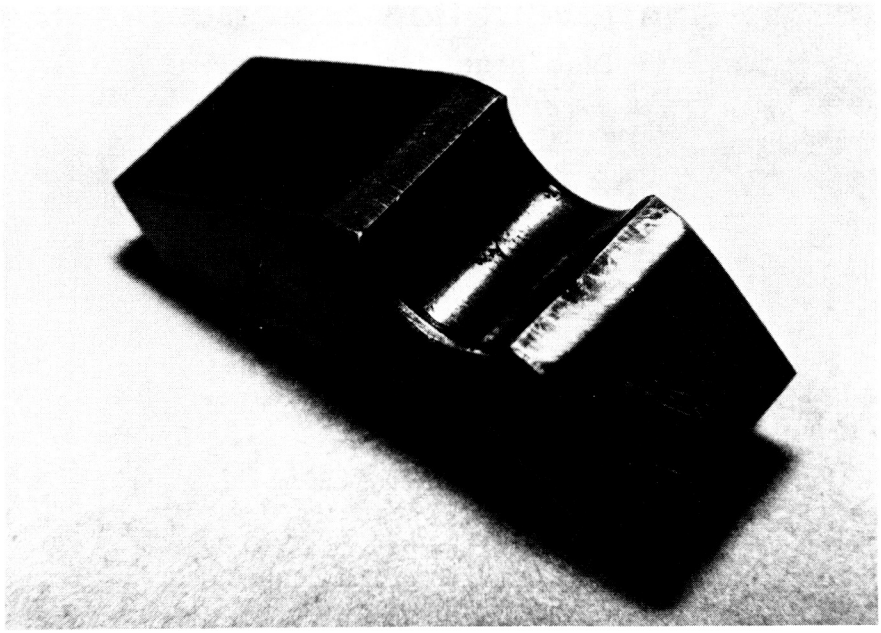

Figure 5A. Photograph of Bearing Pivot Wear Pattern

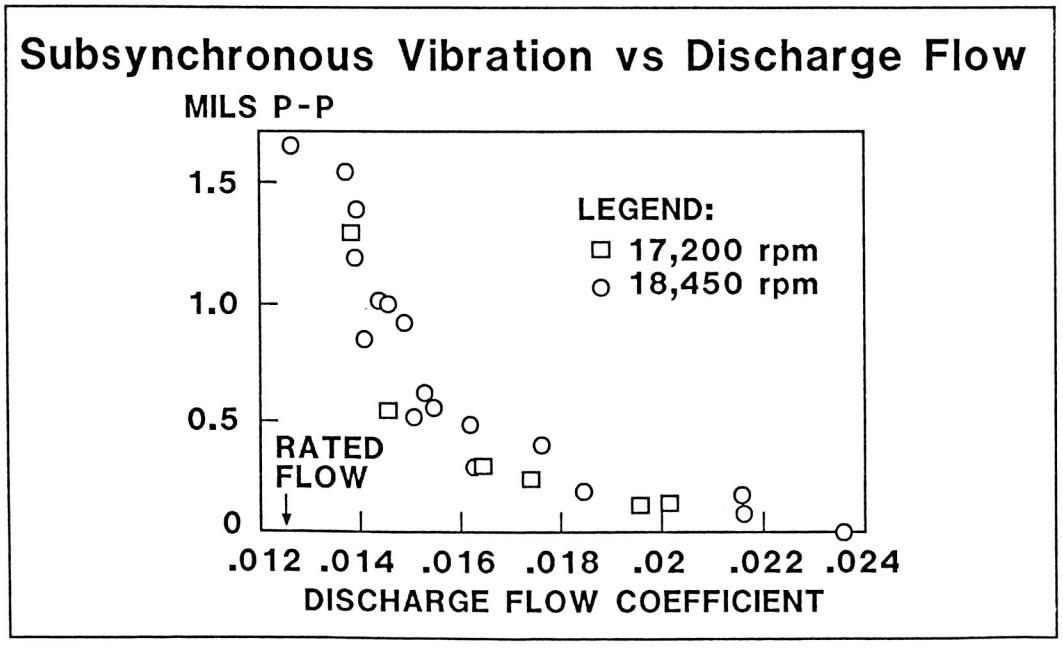

Figure 6. Correlation of Vibration with Discharge Flow

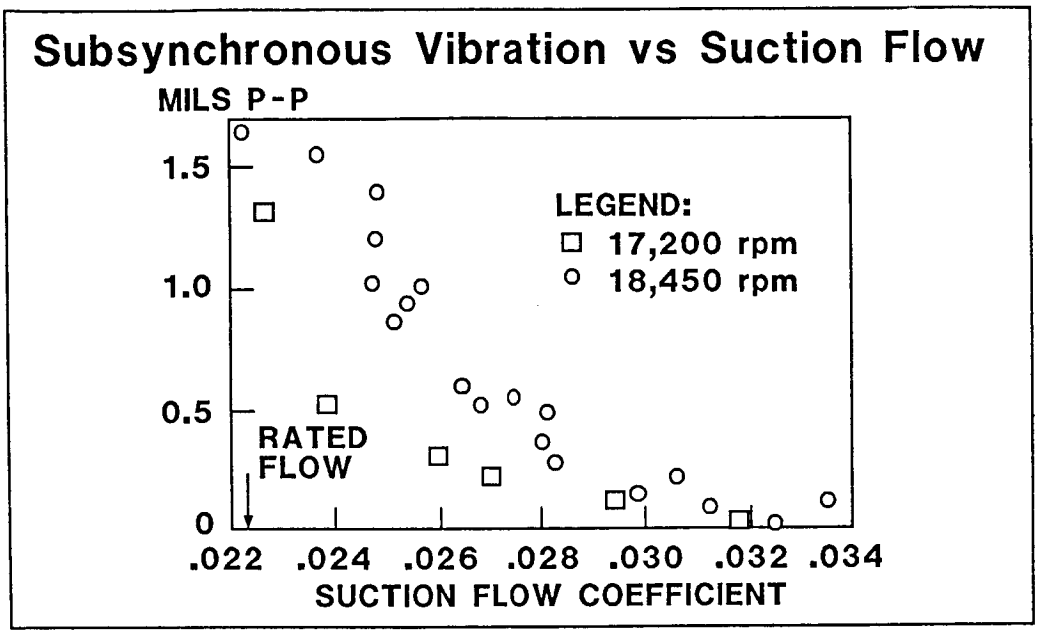

Figure 7. Correlation of Vibration with Suction Flow

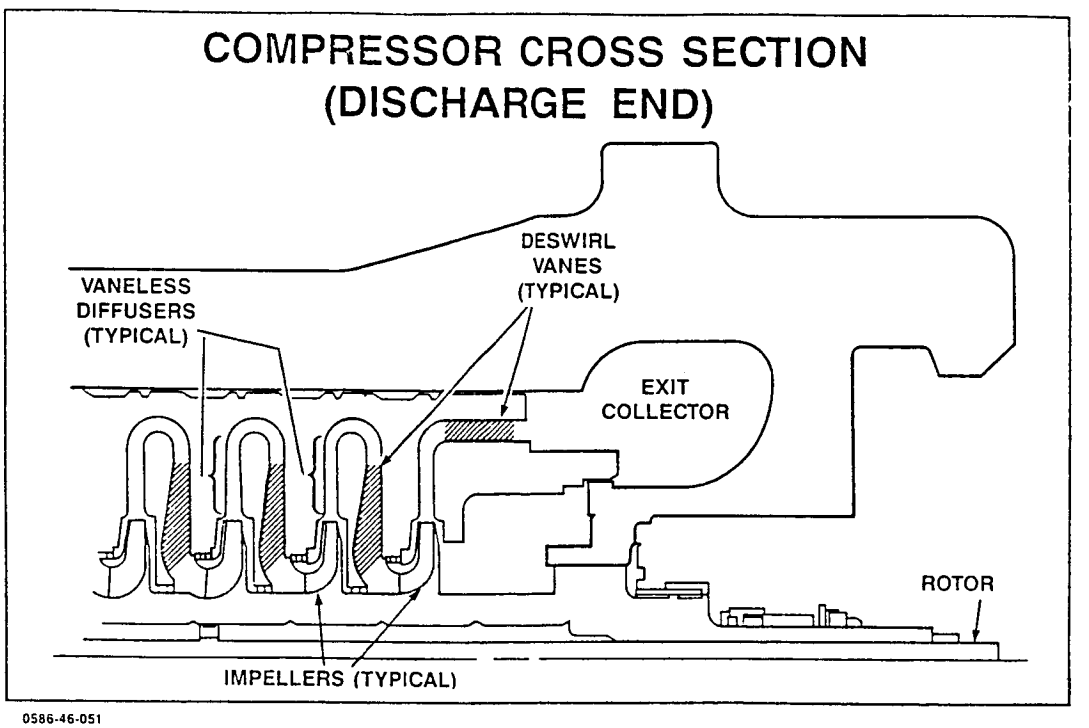

Figure 8. Compressor Cross Section (Discharge End)

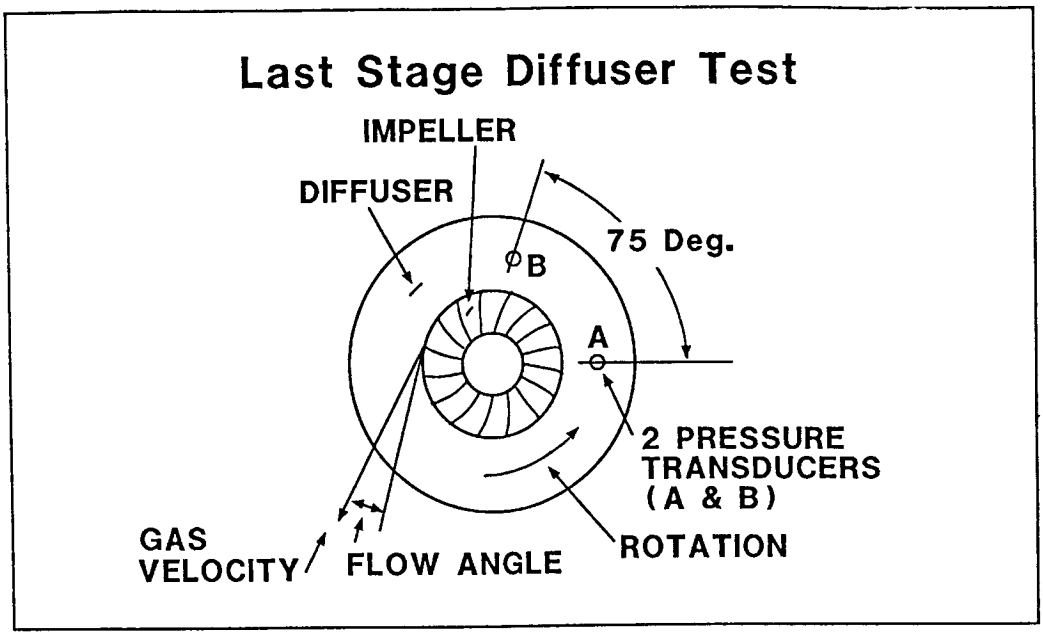

Figure 9A. Factory Test Arrangement

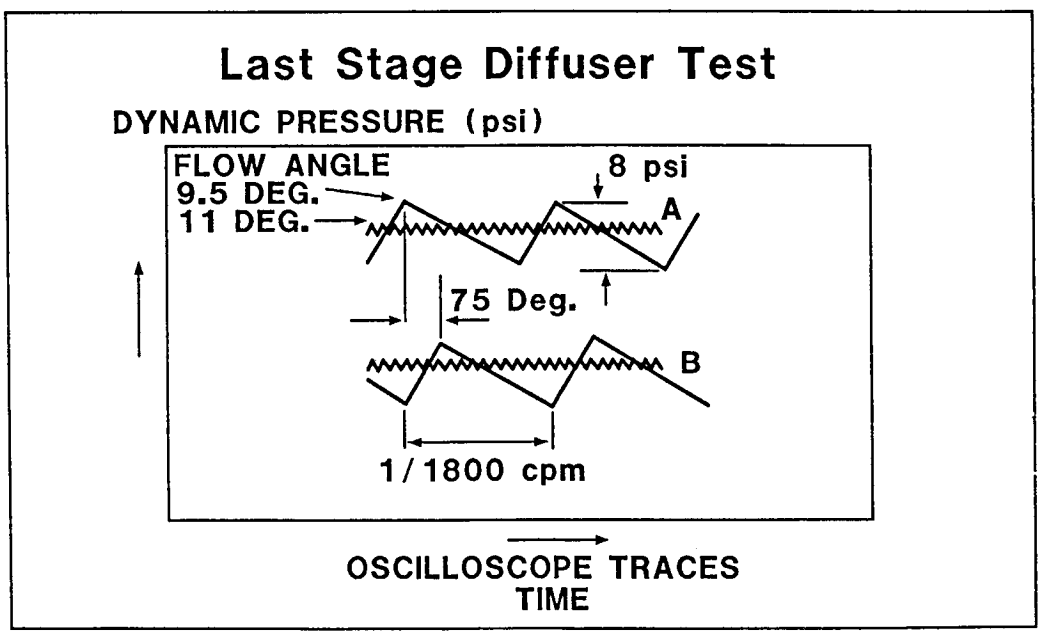

Figure 9B. Factory Test with Diffuser Wall Pressure versus Time

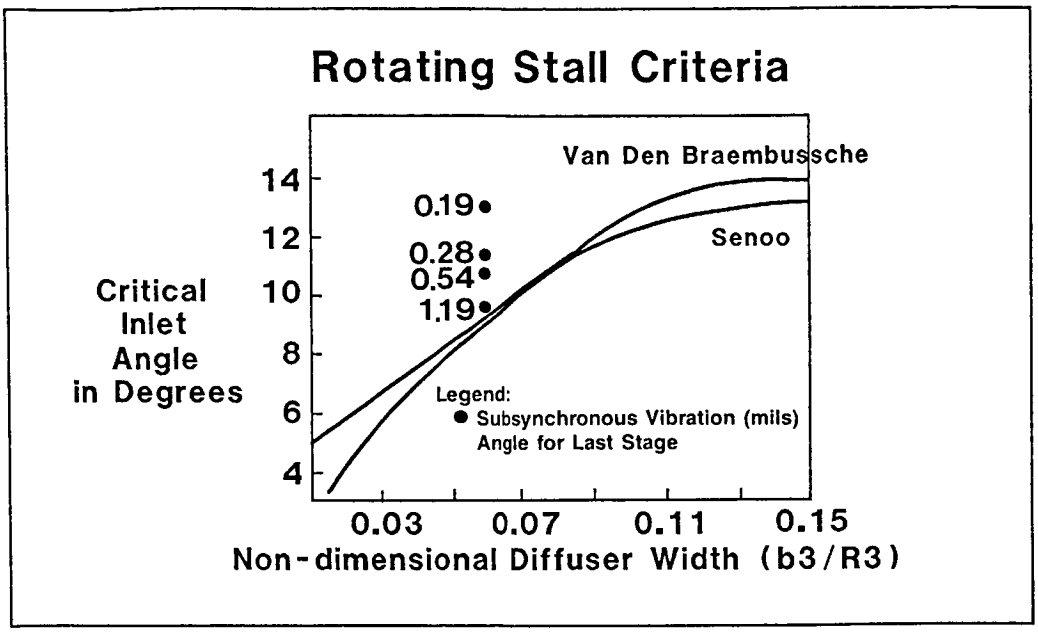

AGXF586-35

Figure 10. Rotating Stall Criteria Compared to Field Test

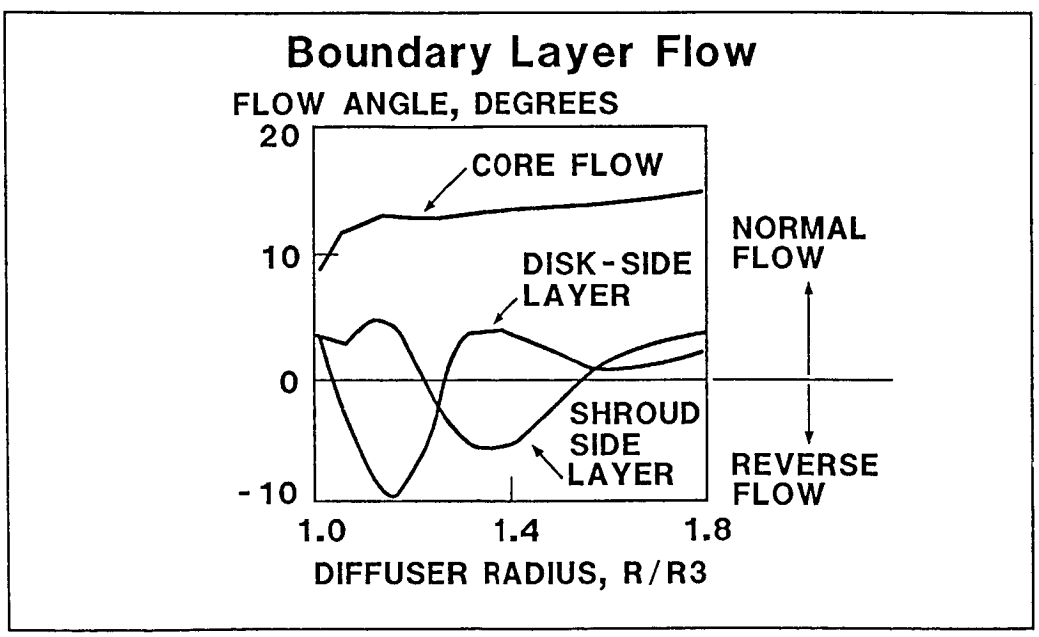

AGXF586-11-16

Figure 11. Diffuser Boundary Layers (Adapted from Senoo, Ref. 1)

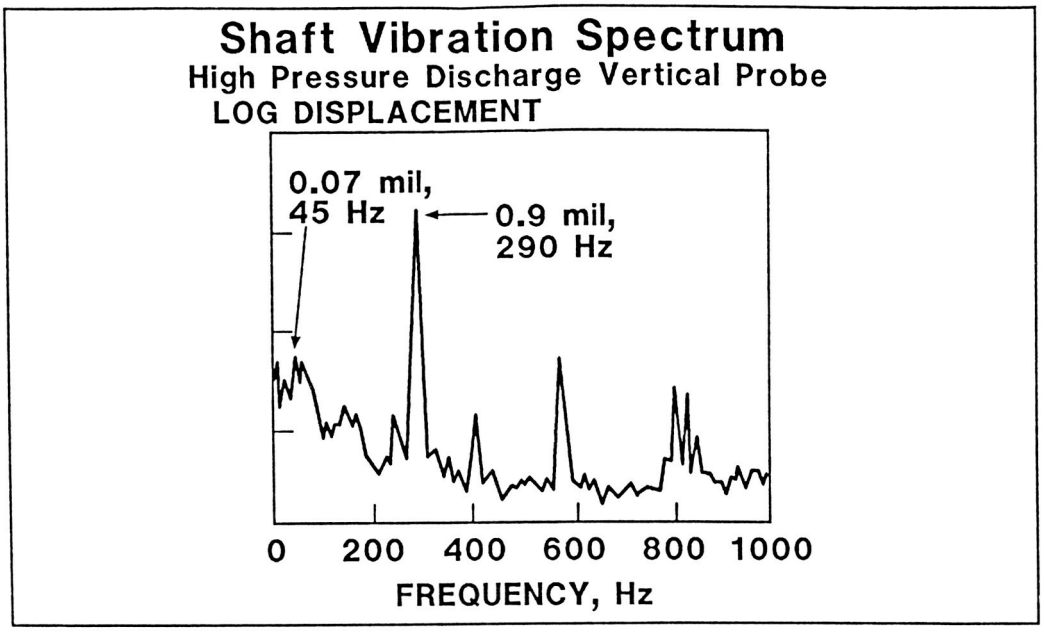

AGXF586-12-18

Figure 12. Spectrum after Modifications

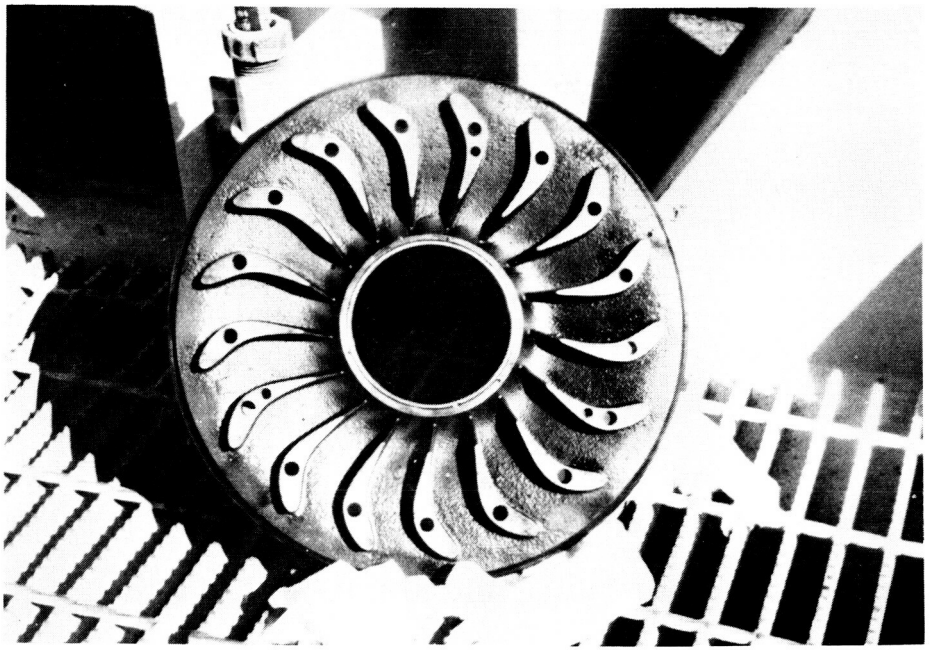

Figure 13. Return Vanes

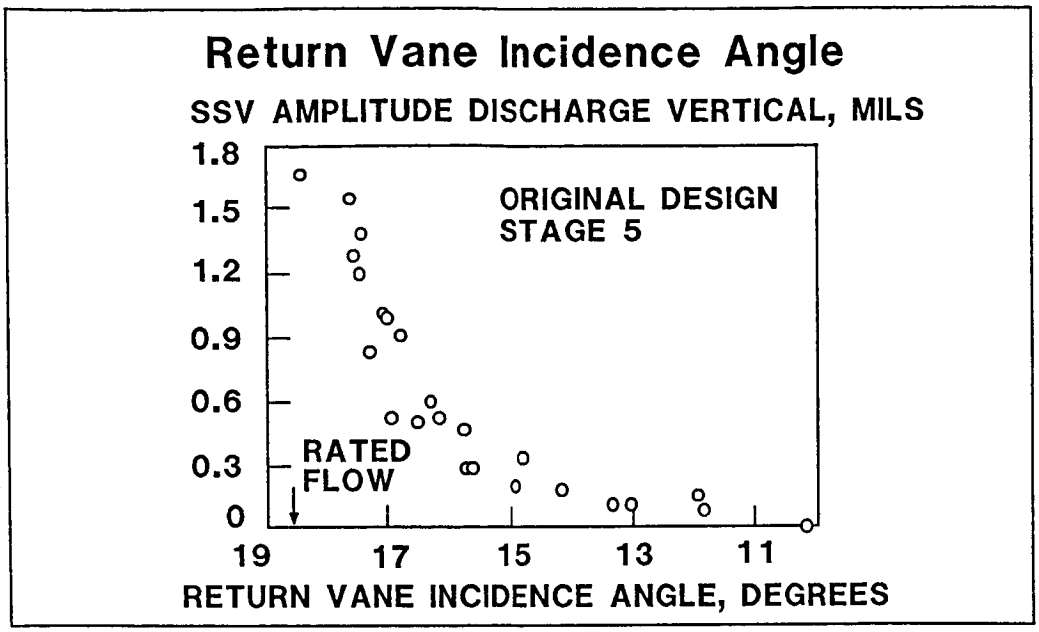

Figure 14. Return Vane Incidence versus Subsynchronous Vibration

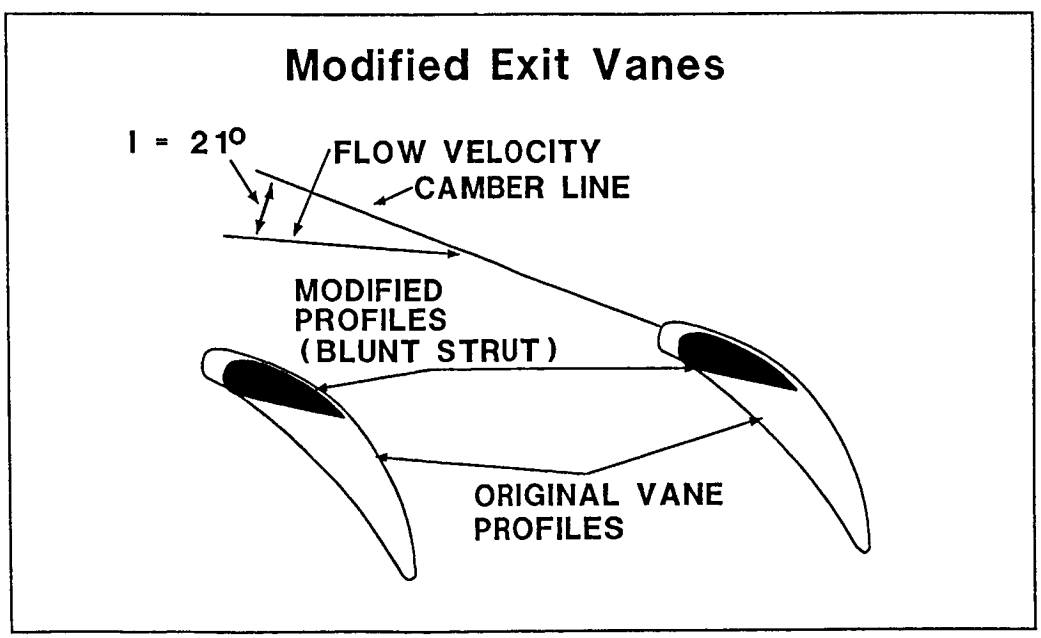

Figure 15. Exit Vane Modification

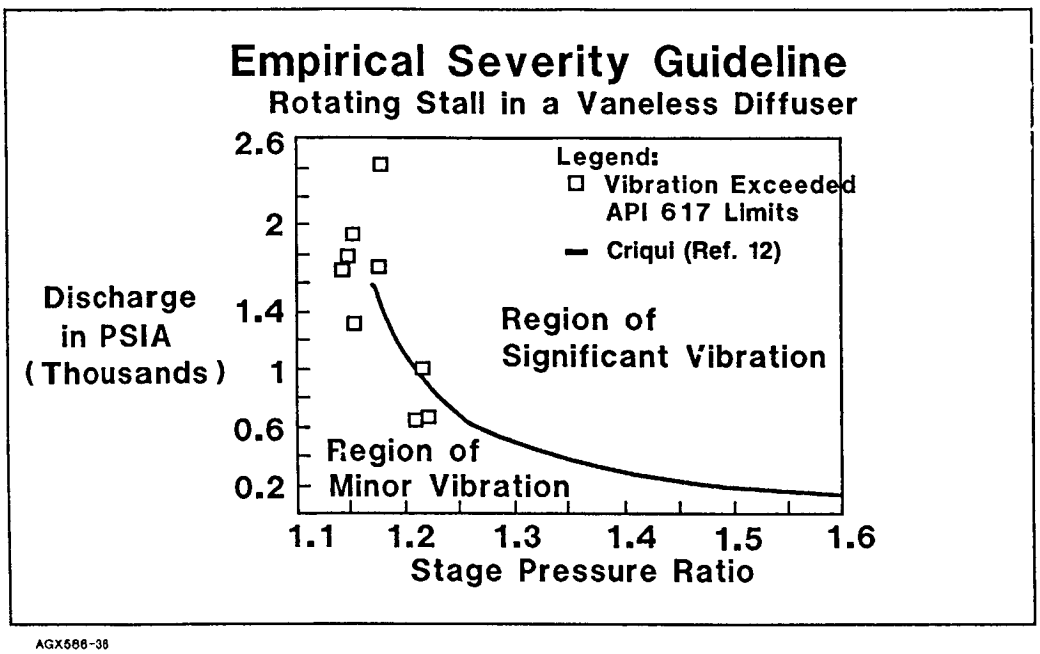

Figure 16. Empirical Severity Guideline